



Progress Highlight

Ground state of the Si(0 0 1) surface revisited—is seeing believing?

T. Uda ^a, H. Shigekawa ^b, Y. Sugawara ^c, S. Mizuno ^{d,e},
H. Tochiwara ^d, Y. Yamashita ^f, J. Yoshinobu ^f, K. Nakatsuji ^f,
H. Kawai ^g, F. Komori ^{f,*}

^a *Advanced Research Laboratory, Hitachi, Ltd., 1-280 Higashi-Koigakubo, Kokubunji, Tokyo 185-8601, Japan*

^b *Institute of Applied Physics, University of Tsukuba, Tsukuba, Ibaraki 305-8573, Japan*

^c *Department of Applied Physics, Graduate School of Engineering, Osaka University, 2-1 Yamada-oka, Suita 565-0871, Japan*

^d *Department of Molecular and Material Sciences, Kyushu University, Kasuga, Fukuoka 816-8580, Japan*

^e *PRESTO, Japan Science and Technology Agency, 4-1-8 Honcho Kawaguchi, Saitama 332-0012, Japan*

^f *Division of Nanoscale Science, The Institute for Solid State Physics, The University of Tokyo, 5-1-5 Kashiwanoha, Kashiwa, Chiba 277-8581, Japan*

^g *Department of Physics, Faculty of Sciences, Kyushu University, Ropponmatsu, Fukuoka 810-8560, Japan*

Abstract

The stable structure of clean Si(0 0 1) surface around 100 K is the $c(4 \times 2)$ arrangement constructed by buckled dimers. This structure was widely accepted as the ground state in 1990's. The view was challenged at the beginning of 2000's by the observations of a $p(2 \times 1)$ structure below 20 K with scanning tunneling microscopy (STM). Recent experimental studies confirm that the dimer is buckled below 30 K. Large tip–surface interaction, and/or tunneling current induced dynamical effect are now experimentally evident in the STM images at low temperatures. Moreover, a current induced structure transformation is discovered below 40 K even in the study by low energy electron diffraction. Dynamical electronic and vibrational effects are theoretically studied for accounting the observation of a $p(2 \times 1)$ structure below 20 K.

© 2004 Elsevier Ltd. All rights reserved.

* Corresponding author. Tel.: +81 4 7136 3310; fax: +81 4 7136 3474.
E-mail address: komori@issp.u-tokyo.ac.jp (F. Komori).

PACS: 68.35.Bs; 68.35.Ja; 68.37.Ef

Keywords: Surface structure; Low temperature; Silicon; Germanium; STM; AFM; LEED; PES

Contents

1. Introduction	148
2. Theoretical overview	149
3. STM observations below 50 K	151
4. Noncontact AFM observations	152
5. Electron beam irradiation effect in LEED measurements of Si(0 0 1) below 40 K	154
6. Evidence of asymmetric dimers of the Si(0 0 1) surface at low temperature by high resolution Si 2p photoelectron spectroscopy	156
7. Reversible and local transformation between $c(4 \times 2)$ and $p(2 \times 2)$ on a Ge(0 0 1) surface	157
8. Vibration of the dimer on the Si(0 0 1) surface excited by STM current	159
9. Concluding remarks	161
References	161

1. Introduction

After the discovery of $p(2 \times 1)$ superstructure of the Si(0 0 1) surface [1], the reconstruction of the surface has been extensively investigated both experimentally [2–11] and theoretically [12–21]. A reversible second-order phase transition between the disordered $p(2 \times 1)$ and ordered $c(4 \times 2)$ phases occurs at ~ 200 K in low-energy electron diffraction (LEED) measurements on the Si(0 0 1) surface [2,3], and the most stable phase was concluded to have the $c(4 \times 2)$ structure. According to scanning tunneling microscopy (STM) studies between 80 and 140 K [4–8], the $c(4 \times 2)$ structure was confirmed to be the most stable arrangement of the buckled dimers at this temperature range. Chadi [12] has found from energy minimization calculations that the asymmetric dimer due to buckling lowers the total energy. The buckling is accompanied with a charge transfer from the lower atom to the upper atom of the dimer. This was consistent with the core level photoelectron spectra suggesting that two types of surface atoms exist [10]. All these results seemed to have settled the controversy about the ground state of Si(0 0 1), and the $p(2 \times 1)$ phase observed

by STM at room temperature was attributed to the quick flip-flop motion of the buckled dimers [17,22,23]. In the previous calculations, the total energy difference between $c(4 \times 2)$ and $p(2 \times 2)$ is 1.2 meV/dimer [18]. From these studies, it was widely accepted that the buckled dimers construct a $c(4 \times 2)$ structure as the ground state.

In recent studies on the low-temperature phase of Si(0 0 1) by STM and atomic force microscopy (AFM), however, $c(4 \times 2)$, $p(2 \times 2)/c(4 \times 2)$, and symmetric dimer images have been observed below 80 K [7,24–28]. These experimental results have questioned the generally accepted picture of the buckled dimer with a $c(4 \times 2)$ ordering as the ground state of the Si(0 0 1) surface. A similar structural change was also suggested by LEED measurements below 40 K [29]. It has been argued from the early stage of the STM observations that strong tip–surface interaction in STM might change the real structure [30]. Thus, several independent groups have studied the surface using other experimental techniques at low temperatures in addition to further STM observations. The ground state and the tip–surface interaction have been also theoretically investigated again. Now it is evident that the tip–surface interaction makes the image of the buckled-dimer symmetric.

In this article, the latest progress of the research on this subject is reviewed. First we briefly summarize the theoretical studies on this surface, and then discuss the structures observed by STM below 50 K. In the STM study [27], both the $c(4 \times 2)$ and $p(2 \times 2)$ structures are observed depending on doping species, temperature and the sample bias voltage. In Sections 4–6, structural studies by AFM at 5 K [26], by LEED down to 24 K, and by Si-2p photoelectron spectroscopy down to 30 K [31] are described. All the results indicate the buckled dimer. Moreover, the $c(4 \times 2)$ structure is suggested as the ground state below 40 K by LEED. The transitions between $c(4 \times 2)$ and $p(2 \times 2)$ induced by tunneling current in STM is described for the clean Ge(0 0 1) surface below 80 K [32] in Section 7. A similar interaction is expected on the Si(0 0 1) surface. In Section 8, vibrational excitation of the dimers by STM current is proposed as a possible origin of its symmetric image on the Si(0 0 1) surface.

2. Theoretical overview

Nearly half century ago, Schlier and Farnsworth [1] observed a $p(2 \times 1)$ structure in a LEED experiment. This is caused by surface atoms moving together in pairs to form dimers. The formation of dimers eliminates one of the two dangling bonds (DB) per surface atom, thereby lowering the surface energy. On the basis of various experimental studies, the $c(4 \times 2)$ reconstruction was suggested as the ground state structure.

Theoretical studies, on the other hand, took off two decades later. In 1978 Chadi demonstrated that buckled dimers are favored through empirical tight-binding method [12]. The DB on the upper dimer atom is an sp^3 orbital with larger s-component and accordingly has lower energy, while that on the lower dimer atom is of

p-character with higher energy. The buckling is caused when energy gain due to charge transfer from the higher to the lower levels is greater than the energy cost due to on-site Coulomb energy, compensated by the Madelung energy. More sophisticated first-principles calculation based on the density functional theory (DFT) by Yin and Cohen [13] confirmed on a 2×1 unit cell that an asymmetric dimer is favored to a symmetric dimer.

Since 1985 when Car and Parrinello developed an efficient first principles algorithm, a number of total energy minimization calculations [14–16,18,21] has been performed on the 4×2 unit cell. These agree that the building blocks are buckled dimers, and the direction of buckling alternates along a dimer row. The formation of $p(2 \times 2)$ or $c(4 \times 2)$ corresponds to adjacent rows in phase or out of phase orientations. In order to obtain conclusive result for the subtle stability difference between $c(4 \times 2)$ and $p(2 \times 2)$, careful modeling of the surface was required. In most calculations, a repeated slab geometry is adopted. One calculates the total energy by fixing the bottom layer at the bulk position, terminating DBs on that layer by hydrogen atoms. In another method, the innermost two layers are frozen and the outermost layers on each side of the slab are allowed to relax. The layer thickness should be doubled but the calculation is free from the effect of induced dipoles at the bottom layer. Inversion symmetry is imposed to accelerate the computation. In either method, the $c(4 \times 2)$ surface is about 1 meV/dimer lower in energy than the $p(2 \times 2)$ surface [18], when a thick sample is used with at least five layers allowed to relax. Some earlier calculations, which resulted in favor of $p(2 \times 2)$ than $c(4 \times 2)$, used thinner slabs [14]. Thus $c(4 \times 2)$ was accepted as the lowest energy structure in the early 1990's.

This picture was challenged by recent experimental work. The STM studies below 80 K showed that $c(4 \times 2)$ becomes unstable and $p(2 \times 2)$ domains appear [8]. It was reported independently by two groups [24,25] that further cooling below 20 K causes the dimers to appear again symmetric.

Theoretically, electron correlation should be reconsidered carefully because first principles calculations based on DFT may not properly describe its role at present. Healy et al. performed quantum Monte Carlo calculation [33] on large cluster models of the surface, and concluded that buckling remains energetically favorable, undermining the ability of DFT to accurately describe the ground state reconstruction of the Si(0 0 1) surface. Thus the old theoretical conclusion still survives that $c(4 \times 2)$ is the ground state structure and the energy difference with $p(2 \times 2)$ is as small as 1 meV/dimer. The result is supported by the recent experimental work reviewed in the following sections. The coexistence of $c(4 \times 2)$ and $p(2 \times 2)$ is rather natural considering the small energy difference between the two. These two phases can be transformed each other by the tip–surface interaction in STM. In certain conditions the buckled dimer may be observed as symmetric due to this interaction.

On the whole, the experiments at very low temperatures do not contradict the DFT calculations at 0 K. However, this fortuitous agreement brings forward a new serious problem why and how $c(4 \times 2)$ is stabilized again at about 100 K in STM observations. This is left to be explained.

3. STM observations below 50 K

Fig. 1(a)–(c) show typical STM images obtained for the Si(0 0 1) surface (P-dope, 0.01–0.001 Ωcm) at 29, 43 and 50 K, respectively [34]. In this case, $c(4 \times 2)$ (red), $p(2 \times 2)$ (blue), and unstable (gray) dimer areas are seen. Fig. 1(d) and (e) show the magnified topographic and current images of the squared area in Fig. 1(b), respectively. In the current image, unstable dimers are shown as scratched, which indicates that the dimers are flip-flopping during the STM measurement. A remarkable point is that the $c(4 \times 2)$ and $p(2 \times 2)$ structures are dominant at ~ 80 and ~ 10 K, respectively, and they gradually change into the other structure via an unstable disordered structure with temperature as shown in Fig. 1(f). Since a second-order phase transition, the disordered $p(2 \times 1)$ to the ordered $c(4 \times 2)$, exists at ~ 200 K, some additional mechanism may be necessary to explain the appearance of the second structural change below 50 K.

At the transition temperature, the $c(4 \times 2)$ or $p(2 \times 2)$ structure emerges into the $p(2 \times 2)$ or $c(4 \times 2)$ area, respectively, with the introduction of P-defects, which are movable topological defects [6,7,35,36]. The P-defect consists of two adjacent dimers which buckle with the same orientation. It can migrate along a dimer row as one of its two dimers changes the buckling orientation. In addition, there appears to be a high percentage of flip-flopping dimer areas as shown in Fig. 1(f). The appearance of the flip-flopping dimers during the transition directly indicates the instability of

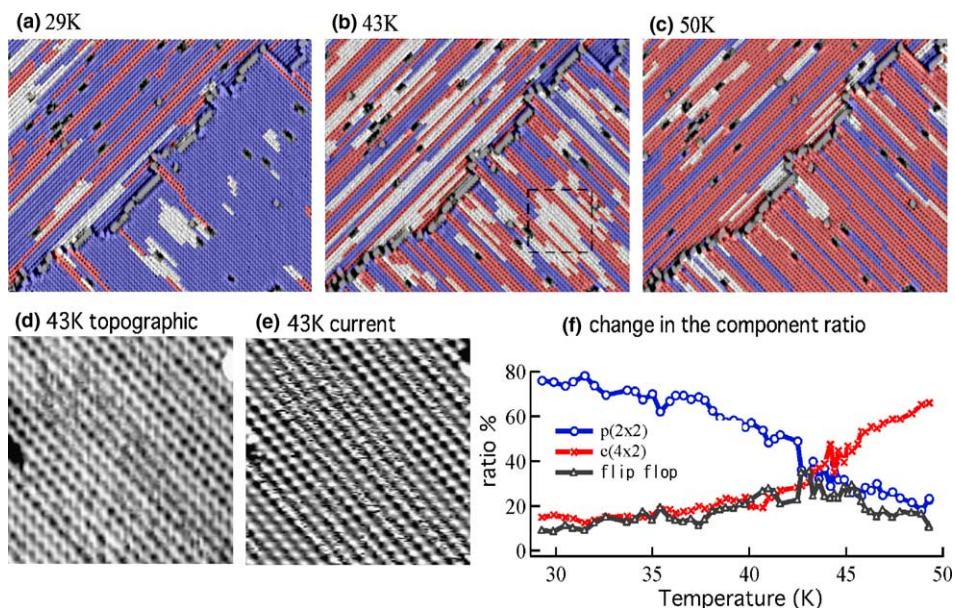


Fig. 1. (a)–(c) STM images for the Si(0 0 1) surface at 29, 43 and 50 K. (d), (e) Magnified topographic (d) and current (e) images of the squared area in (b). (f) Change in the structure components between 29 and 50 K [34].

the buckled dimer structures at these temperatures. The existence of the disorder structure due to the mixture and fluctuation between the $c(4 \times 2)$ and $p(2 \times 2)$ phases indicates that the mutual structural change is easy at the transition temperature, ~ 45 K. If the structure is thermally disordered at 45 K, the barrier height between $c(4 \times 2)$ and $p(2 \times 2)$ should be smaller than that at 80 K.

It is well known that the dimer structures are stabilized with a delicate balance between the electronic and elastic interactions of dimers [37]. Therefore, a possible explanation is to relate the phenomena to the change in the strain and the carrier density depending on the temperature. These are supposed to play an important role in the change in the interaction.

Recently, the influence of the measurement conditions has been reconsidered in detail [27,30,38,39]. An interesting characteristic is the dopant dependence, namely, a $p(2 \times 2)$ single phase at 10 K more easily appears for a sample with the following attributes: (1) n-type, (2) high doping, and (3) very low defect density [27]. Another important point is the tip-induced effect. At low temperatures, the STM tip comes closer to the sample surface due to the low conductivity of the sample and thus activates the structural change such as the flip-flop motion of buckled dimers [30,38]. In fact the applied bias voltage and tunneling current strongly influence the observed structures [27,39]. The transformation of the $c(4 \times 2)$ structure to $p(2 \times 2)$ is observed at 5 K with increasing the bias voltage from 1.3 to 1.4 V [39]. These effects must be taken into consideration to understand the structural change shown in Fig. 1.

4. Noncontact AFM observations

In all STM experiments of the ground state structures, it is possible that the electric field and/or the tunneling current affect the ground state structure. That is, the motion of the atoms occurs due to an excitation by the electric field of the biased tip and/or due to an energy injection by the tunneling current. To investigate the ground state structure, it is necessary to remove tip-induced excitation effect. Non-contact AFM is an alternative tool for high-resolution imaging, which is expected not to cause such excitation effects and therefore to be suitable for observing the ground state structures. This is because the operation of the noncontact AFM is based on very weak interactions due to attractive atomic forces, rather than the electric field utilized in the STM.

Uozumi et al. [26] have experimentally investigated the ground state structure of the Si(0 0 1) surface at 5 K by using noncontact AFM. As force sensors, a conductive Si cantilever was used with a sharpened tip. Its mechanical resonant frequency was 170 kHz. The Si tips were cleaned by Ar-ion sputtering for 30 min, and the native oxide layer and any contamination on the tip apex were removed. Thus, there are dangling bonds out of the Si tip. The frequency modulation detection method was used to measure the force between the Si tip and the Si(0 0 1) surface.

Fig. 2 shows a noncontact AFM image of the Si(0 0 1) surface measured at 5 K. The frequency shift of the cantilever was set at -6 Hz, its vibration amplitude was 17

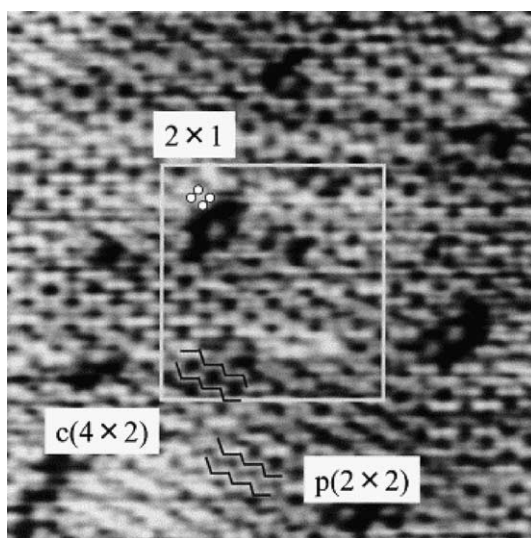


Fig. 2. Noncontact AFM image of the Si(100) surface at 5 K [26]. The scan size is $18.8 \text{ nm} \times 18.8 \text{ nm}$.

nm, and the scan area was $18.8 \text{ nm} \times 18.8 \text{ nm}$. In this image, a bright spot expresses a Si atom at the surface. More than 70% of surface shows the buckled dimers where bright spots form a zigzag pattern. The $c(4 \times 2)$ structure with antiparallel zigzag pattern occupied 61% of all surface, and $p(2 \times 2)$ structure with parallel zigzag pattern occupied only 12% of all surface. This surface has a defect density of 8%. The

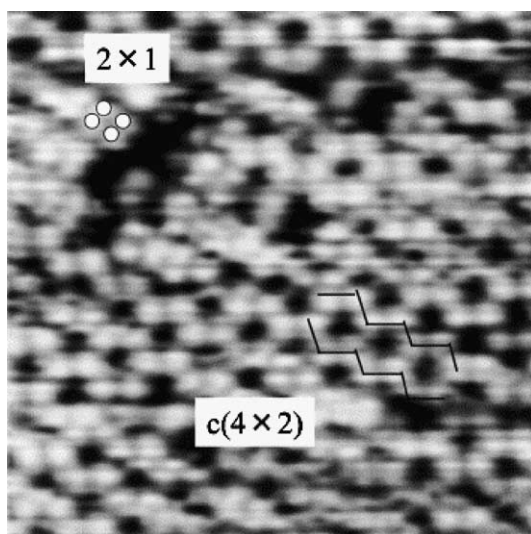


Fig. 3. Noncontact AFM image of the Si(100) surface at 5 K [26]. The scan size is $9.4 \text{ nm} \times 9.4 \text{ nm}$.

observed fuzzy area is as large as 19% because the surface structure shows varieties and becomes vague near defects.

Fig. 3 shows a magnified image of the square area in Fig. 2. The scan area was $9.4 \text{ nm} \times 9.4 \text{ nm}$. Buckled dimers with the $c(4 \times 2)$ structure are confirmed more clearly in this figure. Thus the noncontact AFM study at 5 K indicates that the ground state structure of the Si(0 0 1) surface is the $c(4 \times 2)$ structure.

5. Electron beam irradiation effect in LEED measurements of Si(0 0 1) below 40 K

The STM measurements sometimes cause perturbation on the surfaces, and such effects were confirmed in several experiments [28,30,32,39]. Therefore, it is unclear whether these results reflect intrinsic properties or artifacts. The structure at lower temperatures should be studied by other techniques that would not have a significant influence on the surface structures. LEED was expected to be one of such tools.

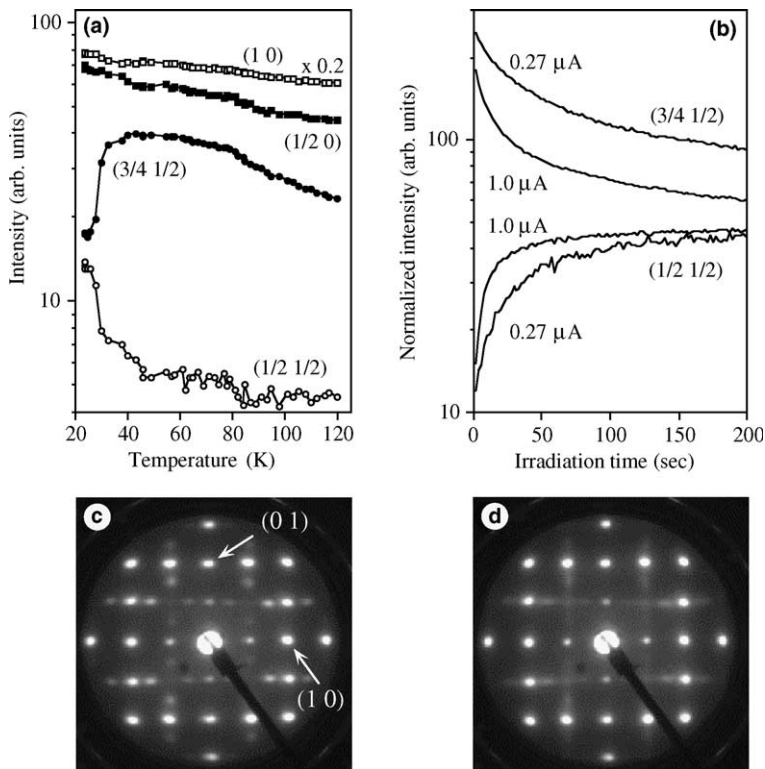


Fig. 4. (a) Spot intensities as a function of sample temperatures ($E_K = 50 \text{ eV}$). (b) Spot intensities as a function of time after a shutter was opened ($E_K = 50 \text{ eV}$). (c) A $c(4 \times 2)$ pattern just after the electron beam irradiation ($0.7 \mu\text{A}$, $E_K = 50 \text{ eV}$) at 24 K. (d) A streaky pattern observed 50 s after the irradiation ($0.7 \mu\text{A}$, $E_K = 50 \text{ eV}$) at 24 K [40].

Matsumoto et al. measured LEED spot intensities as a function of temperature [29]. They obtained the intensity diminution of the quarter-order spots below 40 K. Their results suggested the occurrence of a new order-disorder phase transition at around 40 K. The same change of LEED spot intensities was observed by Mizuno et al. as in Fig. 4. It was concluded [40] that the disappearance of the $c(4 \times 2)$ pattern is caused by the electron beam as described below.

All measurements [40] after the flashing of the surface have been done at pressure less than 3×10^{-11} Torr. The following samples were used: (1) an Sb doped n-type wafer ($0.014 \Omega\text{cm}$), and (2) a B doped p-type wafer ($0.017 \Omega\text{cm}$). Sharp $c(4 \times 2)$ patterns were observed at 80 K. The intensity of the streaks along half-order spots was very weak as observed in the previous LEED study [3]. The $c(4 \times 2)$ structure was determined using LEED $I-V$ analysis at 80 K. The obtained structural parameters were in excellent agreement with the previous theory [21]. There is no difference in structural parameters between samples (1) and (2).

The effect of electron beam irradiation was demonstrated by the following two procedures: (i) The sample position was changed quickly at 24 K during LEED observation; (ii) a shutter between LEED optics and the sample was closed during cooling down to 24 K, and was opened quickly. With both procedures, clear $c(4 \times 2)$ patterns were observed immediately after LEED observation as shown in Fig. 4(c). However, the patterns changed into streaky ones after 50 s at 50 eV and $0.7 \mu\text{A}$ as shown in Fig. 4(d). The same LEED pattern changes were observed for both the p-type and n-type samples.

The procedure (ii) was examined with several electron beam conditions. The intensities of the $(3/4 \ 1/2)$ and $(1/2 \ 1/2)$ spots were plotted in a semi-logarithmic scale with respect to the irradiation time as shown in Fig. 4(b) for sample (2) at 50 eV. The intensities were normalized by the beam current. Initial intensity changes were very rapid and almost completed within ~ 20 s at $1 \mu\text{A}$. Higher beam current resulted in faster changes of the intensities as shown in Fig. 4(b). Very slow changes after 100 s are due to the contamination by residual gases. The slopes of the slow changes did not depend on the beam current but depended on the pressure. The same slow changes were observed at 80 K.

The intensities of some spots were plotted on a semi-logarithmic scale with respect to the sample temperature at incident electron energy of 50 eV in Fig. 4(a). These curves were obtained for sample (2) with increasing temperature by direct heating. At the start of this measurement, the surface was irradiated by electrons for more than 1 min at a sample temperature of 24 K. Therefore, the intensities of the quarter-order spots were already decreased. When the sample temperature rose above 40 K, the intensity of the quarter-order spots recovered and the streaks disappeared. Similar curves were also obtained on cooling. The intensity change of the $(3/4 \ 1/2)$ spot is consistent with the previous ones obtained by Matsumoto et al. [29]. Similar intensity changes were also confirmed for sample (1) and at different electron energies.

We conclude that the most stable structure at 24 K is $c(4 \times 2)$. The intensity changes at 40 K observed in previous LEED study [29] is not a new phase transition but caused by the electron beam irradiation. With increasing irradiation time, the

surface got covered by small $c(4 \times 2)$ and $p(2 \times 2)$ domains at 24 K. This surface quickly rearranged to the well-ordered $c(4 \times 2)$ above 40 K.

6. Evidence of asymmetric dimers of the Si(0 0 1) surface at low temperature by high resolution Si 2p photoelectron spectroscopy

Measurements by STM have larger tip–surface interaction than AFM imaging, and the observed image might differ from the real structure. Therefore, information on core level photoelectron spectroscopy (PES) is useful because it provides chemical states and relative abundance. In addition, core level PES probes information about chemical environment of each atom with an instantaneous excitation.

Yamashita et al. have successfully demonstrated that the up and down dimer atoms, and the subsurface atoms of the clean Si(0 0 1)- $c(4 \times 2)$ surface whose chemical environments are different from that of the bulk produce separate peaks in high resolution Si 2p PES at low temperatures (from 140 to 30 K) [31,41,42]. On the basis of comparison of the Si 2p spectra with the results of STM, it can be clarified whether the symmetric or $p(2 \times 2)$ image in STM is induced by the tip–surface interaction or not.

Fig. 5(a) shows a Si 2p spectrum for the Si(0 0 1) surface at 140 K [41]. In the spectrum, we can decompose the spectrum into five components and assign them: the component B is due to the bulk Si atoms; the components Su and Sd correspond to the up and down Si atoms of the asymmetric dimers, respectively; the component SS is assigned to second-layer Si. The component X is still unidentified. The relative binding energies for Su, X, Sd, and SS to the bulk Si energy position are -485 , -200 , 62 , and 215 meV at 140 K, respectively. The split of 547 meV between the up and down dimer components originates from a substantial charge transfer within the dimer atoms and a final state effect [43]. The peak positions and the angle dependence of intensity ratios agree well with the previous results by Uhrberg group [10].

Fig. 5(a–d) show the Si 2p PES spectra for the Si(0 0 1) surface as a function of temperature ($h\nu = 129$ eV and normal emission) [31,41,42]. As can be seen, the spectral shapes become sharper with decreasing the temperature owing to reduced thermal phonon broadening and/or reduced inhomogeneous broadening. However, the spectral shapes are basically similar, and an additional component is not required for each Si 2p PES spectrum.

Yokoyama and Takayanagi [25] proposed that a dynamical flipping could occur due to the reduced force constant at a low temperature. Shigekawa's group has reported that $c(4 \times 2)$ and $p(2 \times 2)$ coexist on Si(0 0 1) by low temperature STM [27]. If they were intrinsic phenomena, the inhomogeneous broadening of Si 2p peak would be observed. However, this is not the case in the present high resolution Si 2p PES results. Thus, the dimer flipping and/or the formation of $p(2 \times 2)$ ordering is most probably due to induced effects by STM observation. The present Si 2p PES investigation strongly suggests that the buckled dimer with the $c(4 \times 2)$ ordering is stable below 40 K, and the ground state on Si(0 0 1). This is consistent with the results of careful LEED and noncontact AFM studies.

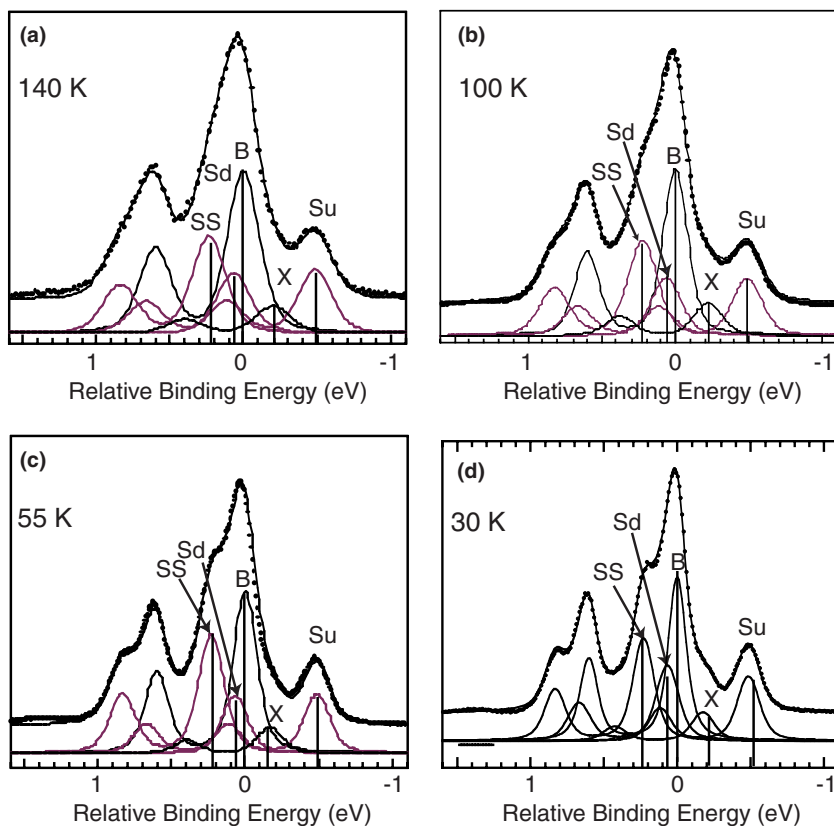


Fig. 5. Si 2p PES spectra for the Si(0 0 1) surface (a) at 140 K, (b) 100 K, (c) 55 K, (d) 30 K [31,41,42]. The emission angle is 0° (normal emission) and the photon energy is 129 eV. B: bulk, Su: up dimer, Sd: down dimer, SS: subsurface, X: unidentified species.

7. Reversible and local transformation between $c(4 \times 2)$ and $p(2 \times 2)$ on a Ge(0 0 1) surface

Reversible control of surface local structures is expected on the $c(4 \times 2)$ reconstructed surface of clean Ge(0 0 1) as well as Si(0 0 1) because the energy difference between the ground state and the $p(2 \times 2)$ structure is estimated to be a few meV/dimer [18,46]. On the both surfaces, the neighboring two atoms form a buckled dimer, and their reconstruction is characterized by the ordering of the buckled dimers. Takagi et al. have reported that the structure can be transformed by changing the sample bias voltage of STM below 80 K on Ge(0 0 1) surface [32,44,45].

The $c(4 \times 2)$ structure is observed with the sample bias $V_b \leq -0.7$ V while $p(2 \times 2)$ with $V_b \geq 0.8$ V at 80 K. Moreover, both structures can be maintained under scanning the surface with $|V_b| \leq 0.6$ V at 80 K after fixing the local structure by scanning there with a higher $|V_b|$. The bias dependence of the surface reconstruction at 80 K is

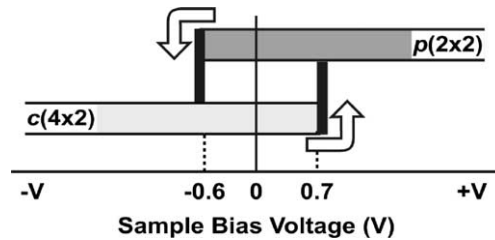


Fig. 6. A schematic showing the observed structures depending on the bias voltage and the direction of the voltage change [32,44].

summarized in Fig. 6. The transformation rate from $c(4 \times 2)$ to $p(2 \times 2)$ at $V_b = 0.8$ V is estimated to be 3×10^{-11} dimer/electron.

Fig. 7 demonstrates a nanoscale memory effect. These images were observed with $V_b = -0.2$ V. After taking the image shown in Fig. 7(a), the area A in the figure was scanned with $V_b = 0.8$ V to change from $c(4 \times 2)$ to $p(2 \times 2)$. The result is shown in Fig. 7(b). The change along the dimer row continued to the outside of the scanning area. Then the area B in Fig. 7(b) was scanned to form another $p(2 \times 2)$ area as shown in Fig. 7(c). The reverse change from $p(2 \times 2)$ to $c(4 \times 2)$ was done by scanning the area C in Fig. 7(c) with $V_b = -0.7$ V. In this case, all of the desired $p(2 \times 2)$ area was scanned because the change to $c(4 \times 2)$ was limited nearby the area of the scanning even along the dimer row. The annihilation of $p(2 \times 2)$ is shown in Fig. 7(d).

It has been argued that the ground state energy of Ge(0 0 1) surface is determined by the two competing energies between the electrostatic energy among the electric dipole moments at the dimers and the subsurface strain energy. When the surface is positively biased under the STM tip, the negatively charged upper-atoms of the dimers are electro-statically pushed toward the subsurface by the tip, and the

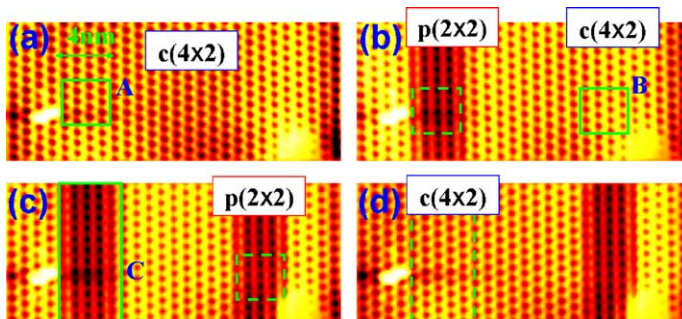


Fig. 7. Successive STM images of the same area (22.5×10 nm²) of a Ge(0 0 1) surface at 80 K [32]. The square areas “A” in (a) and “B” in (b) were scanned with $V_b = 0.8$ V to change the local structure from $c(4 \times 2)$ to $p(2 \times 2)$ after taking each image. The surface after scanning “A” is shown in (b), and that after scanning “B” is in (c). The rectangular area “C” in (c) was scanned with $V_b = -0.7$ V to change it from $p(2 \times 2)$ to $c(4 \times 2)$. The surface after scanning the area “C” is shown in (d).

lower-atoms of the dimers are pulled toward the vacuum side. Consequently, the dimer buckling becomes smaller. This makes the difference of the subsurface strain energy between $c(4 \times 2)$ and $p(2 \times 2)$ structures smaller than that of the dipole energy among buckled dimers. Thus for the positively biased surface, the $p(2 \times 2)$ structure is favored by the gain of the dipole energy, and can be the ground state. On the other hand, under the negative V_b , the buckling of the dimers is increased by the electric field, and the $c(4 \times 2)$ structure is more favored.

The local and reversible restructuring of the Ge(0 0 1) surface is demonstrated between $c(4 \times 2)$ and $p(2 \times 2)$ by controlling the sample bias voltage of STM below 80 K. The ground state can be altered by electric field from the STM tip, and the tunneling current induces the transformation of the structure. There should be the similar STM tip-effect on the Si(0 0 1) surface. The structure change on the Si(0 0 1) surface, however, is observed only when the tunneling current is small [39]. The atomic force between the tip and the surface may influence the structure in the case of the short tip–surface distance.

8. Vibration of the dimer on the Si(0 0 1) surface excited by STM current

The ground state of the Si(0 0 1) surface with the $c(4 \times 2)$ ordered structure of the dimer arrangement turns into a disordered state at room temperature [18,20,21]. In the disordered state, the symmetric images of the $p(2 \times 1)$ structure are observed by STM, and have been attributed to the rapid repeat of the flip-flop motion. Even in the ordered state, the symmetric STM images of the $p(2 \times 1)$ structure [24,25,27] are also observed at some conditions of the tip bias voltages V_b and the STM currents I_{STM} in STM observations at very low temperatures, for example, $V_b = 1$ V and $I_{\text{STM}} = 50$ pA on a boron doped (B-doped) substrate at 5 K [25]. These observations of the symmetric images in the ordered state are puzzling and have not been explained so far.

Kawai and Narikiyo [47] have investigated theoretically the vibration of the dimer excited by the STM current on the Si(0 0 1) surface of the p-type substrate, and have solved the puzzle of the symmetric–asymmetric crossover in the dimer images. They treated the case that V_b is positive and so large that the Fermi level in the conduction band of the STM tip is below the bottom of the π -band. The Hamiltonian used by Kawai and Narikiyo consists of the term of the electronic system describing the tunneling current of electrons from the π -band on the Si(0 0 1) surface to the conduction band of the STM tip, and the electron–vibration coupling term. The latter is the key ingredient. The electron–vibration coupling constant is obtained by the energy of the vibrational state and the model potential for the dimer system on the Si(0 0 1) surface [47,48].

The transition rates σ_{elas} and $\sigma_{0 \rightarrow 1}^{\text{int}}$ for the inter-band transition of electrons from the π -band to the conduction band of the tip are obtained for the elastic transition without coupling to the vibration and for the inelastic transition with the excitation in the vibrational state from the vibrational number $n = 0$ to $n = 1$, respectively. σ_{elas} and $\sigma_{0 \rightarrow 1}^{\text{int}}$ depend critically on I_{STM} and not on the temperature T of the substrate.

The ratio of the rates of the inter-band transition $W = \sigma_{0 \rightarrow 1}^{\text{int}} / \sigma_{\text{elas}}$, however, is shown not to depend on I_{STM} and is given dominantly from the intrinsic property of the Si(0 0 1) surface [47]. The key quantity W is obtained to be about 0.6 from the estimation of the electron–vibration coupling constant and the results of scanning tunneling spectroscopy [25].

At finite temperatures, the deexcitation of the vibrational number through the inner-band excitation of the electron–hole pair creation in the π -band can occur. The rate of the deexcitation $\sigma_{1 \rightarrow 0}^{\text{inn}}$ of vibration through the inner-band excitation is independent of I_{STM} and depends on T [47].

The total transition rates of the excitation $R_{0 \rightarrow 1}$ of the vibrational number $n = 0$ to 1 and the deexcitation $R_{1 \rightarrow 0}$ of that $n = 1$ to 0 are obtained selfconsistently with σ_{elas} , $\sigma_{0 \rightarrow 1}^{\text{int}}$, $\sigma_{1 \rightarrow 0}^{\text{inn}}$, and I_{STM} [47]. The total transition rates $R_{0 \rightarrow 1}$ and $R_{1 \rightarrow 0}$ for B-doped substrate are monotonically increasing as a function of T and I_{STM} in highly nonlinear manner [47]. The distribution of the vibration is well characterized by the effective temperature T_{ef} of the dimer vibration; $T_{\text{ef}} = -\hbar\omega / (k_{\text{B}} \log(R_{0 \rightarrow 1} / R_{1 \rightarrow 0}))$. T_{ef} for B-doped substrate is shown in Fig. 8 [47]. Below 20 K, T_{ef} scarcely depends on T and increases steeply with I_{STM} . T_{ef} becomes about 250 K at $I_{\text{STM}} = 50$ pA and reaches about 400 K at $I_{\text{STM}} = 130$ pA. These high T_{ef} appearing below 20 K, essentially explain why the symmetric STM images are observed at low temperatures. When T increases around 20 K, T_{ef} starts to decrease steeply, because of steep increase of $R_{1 \rightarrow 0}$. T_{ef} increases gradually with T , scarcely depends on I_{STM} , and takes the nearly same values as T . These low T_{ef} explain why the asymmetric STM images recover in the temperature range higher than 50 K.

At temperatures much lower than 20 K, the fraction at the down-position of the atom beneath the STM tip is much larger than that at the up-position, because the tip current and the effective temperature are expected to be much larger and higher at the up-position than at the down-position. The tip height is tuned so that I_{STM} will

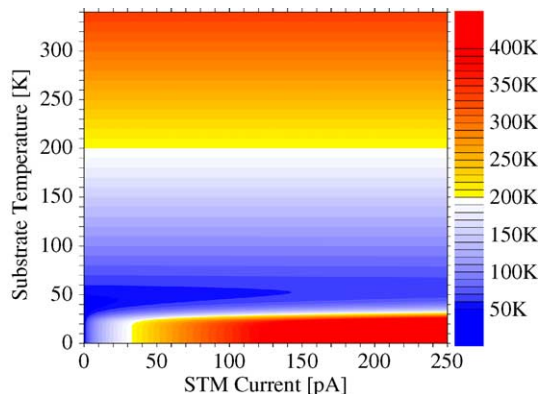


Fig. 8. The effective temperature of the dimer vibration (T_{ef}) on the B-doped substrate [47]. T_{ef} reaches about 400 K for the STM current $I_{\text{STM}} = 130$ pA at low substrate temperatures $T < 20$ K, and decreases steeply around $T \approx 20$ –40 K as T increases.

take the intended value at the down-position. As a result of the large fraction at the down-position, the symmetric dimer images of $p(2 \times 1)$ structure is observed even in the ordered state of $c(4 \times 2)$ at very low temperatures. The crossover behavior on the STM images is semi-quantitatively understood by the nonlinear dependence of T_{ef} on T and I_{STM} [47].

9. Concluding remarks

It is now experimentally clear that the dimers on the Si(0 0 1) surface are buckled at the ground state. The apparent symmetric dimers in STM images are attributed to electronic or vibrational dynamical effects by the tip. A theoretical model including vibrational excitation/deexcitation could explain such phenomena. On the other hand, the ground state ordering of the buckled dimers is experimentally still controversial. The result of the PES study suggests the $c(4 \times 2)$ structure is stable between 80 and 30 K while the change from $c(4 \times 2)$ to $p(2 \times 2)$ is observed in the STM study below 50 K with decreasing temperature. Below 10 K, both the $c(4 \times 2)$ to $p(2 \times 2)$ structures have been reported in the STM observations depending on the doping species and level. Moreover, the structure changes from one to the other by controlling the bias voltage. This indicates that the tip–surface interaction through the current, the electric field and/or the atomic force plays an important role. Further studies are necessary for the understanding of the ground state, the tip–surface interaction and the mechanism of the newly found current effect in the LEED observation below 40 K.

References

- [1] R.E. Schlier, H.E. Farnsworth, *J. Chem. Phys.* 30 (1959) 917.
- [2] T. Tabata, T. Aruga, Y. Murata, *Surf. Sci.* 179 (1987) L63.
- [3] M. Kubota, Y. Murata, *Phys. Rev. B* 49 (1994) 4810.
- [4] R.A. Wolkow, *Phys. Rev. Lett.* 68 (1992) 2636.
- [5] H. Tochiohara, T. Amakusa, M. Iwatsuki, *Phys. Rev. B* 50 (1994) 12262.
- [6] H. Shigekawa, K. Miyake, M. Ishida, K. Hata, *Jpn. J. Appl. Phys.* 36 (1997) L294.
- [7] H. Shigekawa, K. Hata, K. Miyake, M. Ishida, S. Ozawa, *Phys. Rev. B* 55 (1997) 15448.
- [8] K. Hata, M. Ishida, K. Miyake, H. Shigekawa, *Appl. Phys. Lett.* 73 (1998) 40.
- [9] R.J. Hamers, R.M. Tromp, J.E. Demuth, *Phys. Rev. B* 34 (1986) 5343.
- [10] E. Landemark, C.K. Karlsson, Y.-C. Chao, R.I.G. Uhrberg, *Phys. Rev. Lett.* 69 (1992) 1588.
- [11] E.L. Bullock, G. Gunnella, L. Patthey, T. Abukawa, S. Kono, C.R. Natoli, L.S.O. Johansson, *Phys. Rev. Lett.* 74 (1995) 2756.
- [12] D.J. Chadi, *Phys. Rev. Lett.* 43 (1979) 43.
- [13] M.T. Yin, M.L. Cohen, *Phys. Rev. B* 24 (1981) 2303.
- [14] M. Needels, M.C. Payne, J.D. Joannopoulos, *Phys. Rev. Lett.* 58 (1987) 1765.
- [15] Z. Zhu, N. Shima, M. Tsukada, *Phys. Rev. B* 40 (1989) 11868.
- [16] N. Roberts, R.J. Needs, *Surf. Sci.* 236 (1990) 112.
- [17] J. Dabrowski, M. Scheffler, *Appl. Surf. Sci.* 56–58 (1992) 15.
- [18] K. Inoue, Y. Morikawa, K. Terakura, M. Nakayama, *Phys. Rev. B* 49 (1994) 14774.
- [19] P. Kruger, J. Pollmann, *Phys. Rev. Lett.* 74 (1995) 1155.

- [20] K. Terakura, Y. Yamasaki, Y. Morikawa, *Phase Transit.* 53 (1995) 143.
- [21] A. Ramstad, G. Brocks, P.J. Kelly, *Phys. Rev. B* 51 (1995) 14504.
- [22] T. Sato, M. Iwatsuki, H. Tochiyama, *J. Electron. Microsc.* 48 (1999) 1.
- [23] K. Hata, Y. Sainoo, H. Shigekawa, *Phys. Rev. Lett.* 86 (2001) 3084.
- [24] Y. Kondo, T. Amakusa, M. Iwatsuki, H. Tokumoto, *Surf. Sci.* 453 (2000) L318.
- [25] T. Yokoyama, K. Takayanagi, *Phys. Rev. B* 61 (2000) R5078.
- [26] T. Uozumi, Y. Tomiyoshi, N. Suehira, Y. Sugawara, S. Morita, *Appl. Surf. Sci.* 188 (2002) 279.
- [27] K. Hata, S. Yoshida, H. Shigekawa, *Phys. Rev. Lett.* 89 (2002) 286104.
- [28] M. Ono, A. Kamoshida, A. Matsuura, N. Ishikawa, T. Eguchi, Y. Hasegawa, *Phys. Rev. B* 67 (2003) 201306.
- [29] M. Matsumoto, K. Fukutani, T. Okano, *Phys. Rev. Lett.* 90 (2003) 106103.
- [30] T. Mitsui, T. Takayanagi, *Phys. Rev. B* 62 (2000) R16251.
- [31] S. Machida, Y. Yamashita, M. Nagao, S. Yamamoto, Y. Kakefuda, K. Mukai, J. Yoshinobu, *Surf. Sci.* 532–535 (2003) 716.
- [32] Y. Takagi, Y. Yoshimoto, K. Nakatsuji, F. Komori, *J. Phys. Soc. Jpn.* 72 (2003) 2425.
- [33] S.B. Healy, C. Filippi, P. Kratzer, E. Penev, M. Scheffler, *Phys. Rev. Lett.* 87 (2001) 016105.
- [34] S. Yoshida, T. Kimura, O. Takeuchi, H. Oigawa, H. Sakama, T. Nagamura, H. Shigekawa, *Phys. Rev. B* 70 (2004) in press.
- [35] H. Shigekawa, K. Miyake, M. Ishida, K. Hata, H. Oigawa, Y. Nannichi, R. Yoshizaki, A. Kawazu, T. Abe, T. Ozawa, T. Nagamura, *Jpn. J. Appl. Phys.* 35 (1996) L1081.
- [36] S. Yoshida, O. Takeuchi, K. Hata, R. Morita, M. Yamashita, H. Shigekawa, *Jpn. J. Appl. Phys.* 41 (2002) 5017.
- [37] J. Ihm, D.H. Lee, J.D. Joannopoulos, J.J. Xiong, *Phys. Rev. Lett.* 51 (1983) 1872.
- [38] K. Cho, J.D. Joannopoulos, *Phys. Rev. B* 53 (1996) 4553.
- [39] K. Sagisaka, D. Fujita, G. Kido, *Phys. Rev. Lett.* 91 (2003) 146103.
- [40] S. Mizuno, T. Shirasawa, Y. Shiraishi, H. Tochiyama, *Phys. Rev. B* 69 (2004) R241306.
- [41] Y. Yamashita, M. Nagao, S. Machida, K. Hamaguchi, F. Yasui, K. Mukai, J. Yoshinobu, *J. Electron. Spec. Relat. Phenom.* 389 (2001) 114–116.
- [42] Y. Yamashita, S. Machida, M. Nagao, S. Yamamoto, Y. Kakefuda, K. Mukai, J. Yoshinobu, *Jpn. J. Appl. Phys.* 41 (2002) L272.
- [43] E. Pehlke, M. Scheffler, *Phys. Rev. Lett.* 71 (1993) 2338.
- [44] Y. Takagi, M. Yamada, K. Nakatsuji, F. Komori, *Appl. Phys. Lett.* 84 (2004) 1925.
- [45] Y. Takagi, Y. Yoshimoto, K. Nakatsuji, F. Komori, *Surf. Sci.* 559 (2004) 1.
- [46] Y. Yoshimoto, Y. Nakamura, H. Kawai, M. Tsukada, M. Nakayama, *Phys. Rev. B* 61 (2000) 1965.
- [47] H. Kawai, O. Narikiyo, *J. Phys. Soc. Jpn.* 73 (2004) 417, and references therein.
- [48] H. Kawai, R. Miyata, Y. Yoshimoto, M. Tsukada, *J. Phys. Soc. Jpn.* 72 (2003) 3158, and references therein.